Sequential hydrothermal dechlorination and liquefaction of PVC

Energy Conversion and Management 304 (2024) 118228

Contents lists available at ScienceDirect

Energy Conversion and Management

journal homepage: www.elsevier.com/locate/enconman

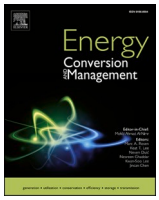

Sequential hydrothermal dechlorination and liquefaction of PVC

Edoardo Tito [a], Juliano Souza dos Passos [b], Alessandro Girolamo Rombolà [c], Cristian Torri [c], Samir Bensaid [a], Raffaele Pirone [a], Patrick Biller [b,*]

[a] Department of Applied Science and Technology, Politecnico di Torino, Corso Duca degli Abruzzi 24, 10129, Turin, Italy
[b] Biological and Chemical Engineering, Aarhus University, Hangøvej 2, DK-8200 Aarhus N, Denmark
[c] Department of Chemistry "Giacomo Ciamician", University of Bologna, Via Sant'Alberto 163, 48123, Ravenna, Italy

ARTICLE INFO

Keywords:
Poly(vinyl chloride)
PVC dechlorination
Chlorine
Two-stage hydrothermal liquefaction
Chemical recycling

ABSTRACT

Poly(vinyl chloride) (PVC) is globally the third most produced plastic, but recycling PVC waste through mechanical means is difficult. Due to the high presence of chlorine in PVC, it is unsuitable for both pyrolysis and combustion. Consequently, there is a need to explore innovative methods for harnessing its energy potential. Hydrothermal liquefaction (HTL) is a topic of growing interest in the literature for chemical recycling of waste plastic or conversion into liquid energy carriers. In this work an innovative sequential hydrothermal processing strategy was tested for oil production from PVC. PVC at high loadings (20 wt.%) was first processed under subcritical conditions to produce a chlorine-free solid, which was then liquefied in supercritical conditions. Different temperatures were tested for the dechlorination stage, and at 300 °C 99% of chlorine was removed, while 94% of carbon remained in the solid residue. The mechanism behind the solid's formation was investigated by assessing activation energies, both with the addition of KOH as a neutralizing agent (120 kJ/mol) and without it (186 kJ/mol). Different temperatures were screened for an HTL supercritical stage (420–480 °C), but the maximum conversion of the dechlorinated solid was 47%, and the maximum mass yield of oil was 10%. Overall, the subcritical phase demonstrated its potential as a technology for producing chlorine-free solid material with a high energy density. The subsequent supercritical step partially valorized the dechlorinated solid by producing an aromatic-rich oil phase.

1. Introduction

The invention of plastic represented a major technological advance in human history, as it enabled the production of an inexpensive, lightweight, flexible material with easily tailorable properties. For these reasons, since the 1930 s, when the first polymers were invented, the global plastic production has risen up to 359 Mt/yr in 2018 [1]. Given the non-biodegradability of synthetic polymers, the amount of plastic waste has built up since then. As of 2015, 6300 Mt of plastic waste had been generated of which 12% incinerated, 79% disposed in landfills or spread into the environment, and only 9% recycled [2]. A great deal of effort is directed towards improvements in recycling technologies. However limitations are still present when dealing with mixed plastic waste [3,4]. Indeed, mechanical recycling, the cheapest and most common recycling technique, can be used only for pure streams containing only one type of polymer, typically pre-consumer waste or specific post-consumer stream of plastics (e.g. PET bottle) [3]. Moreover, mechanically recycled plastic is generally downgraded to lower-performing uses. From an environmental perspective, for mixed plastic waste that cannot be mechanically recycled, the preferred approach is chemical recycling, followed by energy valorization [5]. The former allows the recovery of materials in the form of chemicals that can be used to produce virgin polymers with the same properties as fossil-derived ones, while the latter allows the recovery of energy while limiting the amount of waste that needs to be disposed of.

Poly (vinyl chloride) (PVC) is currently the third most produced polymer worldwide [6], and in 2015 the PVC waste reached 15 Mt/y, mainly linked to the building and construction sector, which requires 69% of the overall PVC produced [2]. Furthermore, PVC is typically the third most present plastic in the organic fraction of municipal waste [7] and in mixed waste for incineration plants [8]. Given its pervasive presence, addressing PVC waste has become imperative.

As a way of chemically recycling plastic waste, there has been a growing interest towards thermochemical technologies. Specifically,

* Corresponding author.
E-mail address: pbiller@bce.au.dk (P. Biller).

https://doi.org/10.1016/j.enconman.2024.118228
Received 4 January 2024; Received in revised form 17 February 2024; Accepted 19 February 2024
Available online 23 February 2024

processes such as pyrolysis and supercritical hydrothermal liquefaction (HTL) have demonstrated promising outcomes [9–11]. Through them, a consistent amount of carbon present in the mixed plastic waste can be converted into a hydrocarbons-rich gas phase and into an oil that can be used as feedstock for the production of virgin polymers, closing the plastic loop [10,12,13]. However, dealing with even a small quantity of PVC within the plastic mix poses significant technical challenges [3,14]. Indeed, PVC is a halogenated polymer, consisting of a carbon chain containing chlorine side groups accounting for 57% of the overall mass. The release of chlorine during the recycling process results in a substantial increase in acidity, making the reaction environment highly corrosive. This corrosiveness can significantly reduce the operational lifespan of facilities [15], especially under the demanding conditions of pyrolysis [14] and supercritical HTL. Additionally, the presence of chlorine-containing compounds in the resulting oil hampers its subsequent utilization [16,17]. Hence, the prospect of employing a preliminary treatment step to eliminate chlorine from mixed plastic waste emerges as a compelling avenue [17]. This approach could facilitate the subsequent chemical recycling of the waste using a more intensive process.

The pretreatment step could be performed in subcritical environment. It has been observed that while polyolefins and polystyrene require supercritical conditions to react [9,18,19], heteroatoms-containing polymers (e.g. PET, nylon, polyurethane) can be easily hydrolyzed already in subcritical conditions [18,20]. In the same way, PVC at low loadings (~0.15 wt.%) can achieve complete dechlorination in water at around 240 °C [21], resulting in a solid phase with low residual chlorine and an acidic aqueous phase rich in HCl [22,23]. The high acidity of the aqueous medium, besides posing a threat to the material used for the construction of the reactor [24,25], could also be the reason why the production of solid from PVC is predominant in hydrothermal environment and no oil is recovered [22]. Indeed, acidity is well recognized in HTL for increasing the solid yield due to dehydration and repolymerization reactions [26]. For this reason, alkali additives (NaOH, KOH, K_2CO_3) were tested during subcritical dechlorination of PVC [25,27,28]. The results showed that the use of a basic additive could be beneficial for the dechlorination efficiency especially at low reaction temperature. Nevertheless, it was observed that an excessive amount of alkali diminished the positive effect [28]. However, these observations were performed with sub-stoichiometric amounts of additive, and very limited information exists regarding reaction kinetics when employing stoichiometric amounts of base to neutralize all chlorine-derived acidity. Moreover, it would be beneficial to have a neutralizing agent that could decrease the corrosivity of the aqueous media by means pH control, and that the chlorine salt of the base used could be easily recovered downstream of the reaction process.

In this work, we propose to apply a two-stage hydrothermal process to valorize plastic waste with a high concentration of PVC. This innovative process involves a first step in subcritical conditions, taking advantage of PVC's propensity for dechlorination in hydrothermal environment, targeting in a dechlorinated solid and an aqueous phase containing HCl. Experiments were conducted with pure PVC at high loadings (20 wt.%) with and without the addition of an equimolar amount of KOH. The effects of temperature and the use of KOH were studied, focusing on mass yields, residual chlorine, as well as solid properties. The reaction mechanism during the subcritical stage were hypothesized, based on literature data and the obtained experimental results, emphasizing the differences in reaction pathways between the presence and absence of a basic additive. In particular, the activation energy for both the neutralized and non-neutralized cases was evaluated.

Here, we propose the use of a first subcritical stage intended to remove chlorine from plastic waste in order to valorize the resulting solid through the more severe supercritical HTL. For this reason, the dechlorinated solid obtained from the subcritical dechlorination, both in neutralized and non-neutralized cases, was processed in supercritical HTL. Pyrolysis of the dechlorinated solid was also investigated by Py-GC/MS to better characterize its structure, as well as to compare it with supercritical HTL and elucidate the role of water in solid degradation. During supercritical HTL, thermal breakdown of the dechlorinated solid was hypothesized to lead to the formation of lower molecular weight compounds in an oil phase. This way, the two-stage hydrothermal process would enable the production of oil from PVC-containing waste.

2. Materials and methods

2.1. Subcritical reaction stage

Experiments were performed in mini-batch reactors having an internal volume of 20 ml. These were built with 316 stainless steel pipes, as described elsewhere [29]. PVC (low molecular weight) purchased from Sigma-Aldrich was used as feedstock. 1.8 g of PVC were loaded in the reactor along with sufficient distilled water to achieve an overall mass of 9 g. For reactions involving neutralization, 1.8 g of PVC was combined with 1.81 g of KOH (10% excess in molar basis), maintaining the total mass at 9 g. This ensured the neutralization of all HCl produced after complete PVC dechlorination. The reactors were sealed at ambient pressure and then submerged into an FSB 3 Fluidized Sand Bath (Omega Engineering, USA), preheated at set point temperature. Six different temperatures were tested from 200 °C to 325 °C at a 25 °C interval in the case of non-neutralized reactions, and between 250 °C and 300 °C for neutralized reactions. The operating pressure was equal to the autogenous one. The residence time was kept fixed at 20 min, after which the reactor was rapidly cooled in water. It is worth noting that corrosion was observed, also due to the high loading of PVC, and that reactors lasted for few experiments. Samples were labeled based on the operating temperature (e.g., 200, 225, 250, 275, 300, 325), and in the case of neutralized reactions, 'KOH' was appended to the name (e.g., 250-KOH, 275-KOH, 300-KOH). All reactions were performed at least in duplicates.

The mass of gas was quantified by weight difference between the reactor before and after venting. After that, the liquid present in the reactor was poured in a centrifugal tube and centrifugated at 3500 rpm for 5 min. The separated liquid was collected. The solid remaining inside the reactor and in the centrifugal tube was removed by rinsing with distilled water and mechanical action using a spatula. This aqueous solution was vacuum filtered with Buchner funnel and a pre-weighed paper filter. The filter was left overnight in oven at 105 °C to remove residual moisture; it was then weighed and the solid collected.

2.2. Supercritical reaction stage

Reactions were performed in mini-batch reactors having an internal volume of 10 ml. These were composed by a ¾ inch port connectors and cap (Hy-Lok©) made of 316 stainless steel, as described elsewhere [18]. The amount of water loaded in the reactor was calculated based on the vapor pressure of water at the operating temperature in order to have an autogenous pressure of 225 bar. Water amount ranged within 0.832–1.084 g. The solid feedstock used was the dechlorinated sample obtained from the subcritical step; a solid/water ratio of 1/2 was kept fixed. The reactor was then inserted in a pre-heated furnace (Carbolite GSM 11/8 8L) at set point temperature. Four different temperatures were tested from 420 °C to 480 °C with a 20 °C interval. All reactions were performed at least in duplicates. After 60 min in the furnace, reactors were removed and let cool in air. When room temperature was reached, reactors were weighed before and after venting, so gas yield could be determined by difference. The aqueous phase of the reactor was then poured into a beaker and vacuum filtered. The residue inside the reactor, as well as the solid retentate from the filtration, were washed with methanol. The organic solution was vacuum filtered to separate solid and the methanol phase. The filter containing the solid was dried

overnight in an oven at 105 °C to remove residual moisture; it was then weighed and the solid collected. The solid-free methanol solution was collected in a 30 ml amber bottles and left under nitrogen flow until the solvent was completely removed. The residual oil phase was then weighed.

2.3. Analysis

An elemental analyzer (Elementar vario Macro Cube) was used to determine the elemental composition (C, H, N and S) of PVC and solid products. Chlorine determination was performed by μ-XRF (Bruker-Tornado M4). Measurements were performed in duplicate for every sample analyzed. The carbon and chlorine recoveries in the solids were computed according to Eq. (1) and Eq. (2), respectively. The correlation by Channiwala & Parikh (Eq. (3) was used to estimate the Higher Heating Value (HHV) based on elemental composition, as it was checked to be applicable even for materials with high chlorine content like PVC [30]. Chemical Energy Recovery (ER) of products was estimated using Eq. (4).

$$Carbon\,recovery\,(\%) = \frac{Carbon\,content\,solid\left(\frac{kg\,C\,in\,solid}{kg\,solid}\right)\cdot solid\,mass\,yield\left(\frac{kg\,solid}{kg\,PVC}\right)}{Carbon\,content\,PVC\left(\frac{kg\,C\,in\,PVC}{kg\,PVC}\right)} \quad (1)$$

$$Chlorine\,recovery\,(\%) = \frac{Chlorine\,content\,solid\left(\frac{kg\,C\,in\,solid}{kg\,solid}\right)\cdot solid\,mass\,yield\left(\frac{kg\,solid}{kg\,PVC}\right)}{Chlorine\,content\,PVC\left(\frac{kg\,C\,in\,PVC}{kg\,PVC}\right)} \quad (2)$$

$$HHV\left(\frac{MJ}{kg}\right) = 0.3491{\cdot}C\,(wt.\%) + 1.1783{\cdot}H\,(wt.\%) - 0.1034{\cdot}O\,(wt.\%) + 0{\cdot}Cl\,(wt.\%) \quad (3)$$

$$ER(\%) = Product\,mass\,yield\left(\frac{kg\,product}{kg\,PVC}\right)\cdot\frac{HHV_{product}\left(\frac{MJ}{kg}\right)}{HHV_{feedstock}\left(\frac{MJ}{kg}\right)} \quad (4)$$

Thermogravimetric analysis (TGA) was performed on a Mettler–Toledo analyzer (TGA/DSC 3^+). Samples were loaded in 70 μl crucibles which were heated under nitrogen flow (50 ml/min) from 50 to 900 °C with heating rate of 10 °C min^{-1}. Samples were then kept at 900 °C for 10 min under air flow (50 ml/min).

Attenuated Total Reflectance Fourier-transformed infrared spectroscopy (ATR-FTIR) was performed on a Bruker Alpha Platinum spectrometer. 24 spectra from 4000 to 400 cm^{-1} with resolution of 2 cm^{-1} were automatically collected for every sample and the average value was given as result.

Py-GC–MS analyses were performed using a multi-shot pyrolyzer EGA/Py-3030D micro-furnace (Frontier Laboratories Ltd. Fukushima, Japan) interfaced to a gas chromatograph coupled with a mass spectrometer (7890B and 5977B Agilent Technologies, Palo Alto, USA). About 1 mg of each sample was placed into a clean stainless-steel cup, inserted into the micro-furnace and pyrolyzed at 600 °C for 1 min with helium as carrier gas (1 ml min^{-1}). The GC injector was operated at 280 °C, with 1:20 split ratio, and the interface temperature was kept at 280 °C. The pyrolysis products were eluted in constant flow mode at 1 ml min^{-1} (carrier gas helium) and separated by a HP-5MS fused silica capillary column (dimensions 30 m × 0.25 mm × 0.25 μm) with the following temperature program: 50 °C (2 min) // 10 °C min^{-1} // 280 °C (8 min). The MS was operated in EI positive mode (70 eV, scanning 10–600 *m/z*) with transfer line temperature 250 °C, ion source temperature 230 °C and quadrupole temperature 150 °C. Each sample was analyzed in triplicate and blanks were performed before each set of analysis.

The compositions of the oil obtained after the supercritical step was analyzed using a GC–MS (Agilent 7890B GC-Agilent 5977A). After removing the solvent from the oil phase, most of the light phase was lost (Figure S1). Therefore, the characterization of the oil phase was performed by directly injecting the oil-containing solvent without prior solvent removal. For this analysis, instead of using methanol as extracting agent, as typically done during the normal work-up, acetone was utilized. A volume of 1 μl of the acetone solution was directly injected into a VF-5 ms column (dimensions 60 m × 0.25 mm × 25 μm), with a split ratio 20:1 and an injection temperature of 280 °C. The helium flow in the column was kept constant at 1 ml/min while the temperature programming was 40 °C (5 min) // 10 °C/min // 100 °C (0 min) // 4 °C/min // 280 °C (0 min)// 10 °C/min // 300 °C (0 min). Compound identification was based on NIST 17 library.

2.4. Kinetic parameters evaluation

Differential scanning calorimetry (DSC) was performed on a Mettler–Toledo analyzer (TGA/DSC 3^+). PVC samples were loaded in sealed micro-reactors (30 μl) at 20% solid loading. Crucibles were then heated under nitrogen flow (50 ml/min) from 30 to 340 °C at 4 different heating rates 10–20-30–40 °C min^{-1}. At 340 °C the samples stayed for further 20 min.

The Kissinger method was used for the determination of the kinetic parameters [31]. The apparent activation energy (E_A) was evaluated based on the following equation (Eq. (5):

$$ln\left(\frac{\beta}{T_m{}^2}\right) = ln\left(\frac{k_\infty{\cdot}R}{E_A}\right) - \frac{E_A}{RT_m} \quad (5)$$

where β is the heating rates, T_m is the reaction peak temperature, R is the Arrhenius constant, k_∞ is the pre-exponential factor of the Arrhenius constant. Plotting $ln\left(\frac{\beta}{T_m{}^2}\right)$ vs $1/RT_m$ the apparent activation energy of the reaction can be determined by the slope of the line, while the pre-exponential can be determined by the intercept.

3. Results and discussion

3.1. Mass yields

In Fig. 1, the yields of solid residue obtained after the subcritical stage are depicted. With the non-neutralized reactions, a decrease in the solid yield is observed with increasing temperature. At 200 °C almost all the solid remained unconverted, while most of the mass was lost between 225 and 250 °C. Hydrothermal dechlorination of PVC was already observed to take place below 250 °C [21,32], hence the solid loss in this range is attributed to this. By further increasing the operating temperature, the solid yield further decreased to 42% at 300 °C. This value corresponds to the theoretical solid yield obtained if a complete

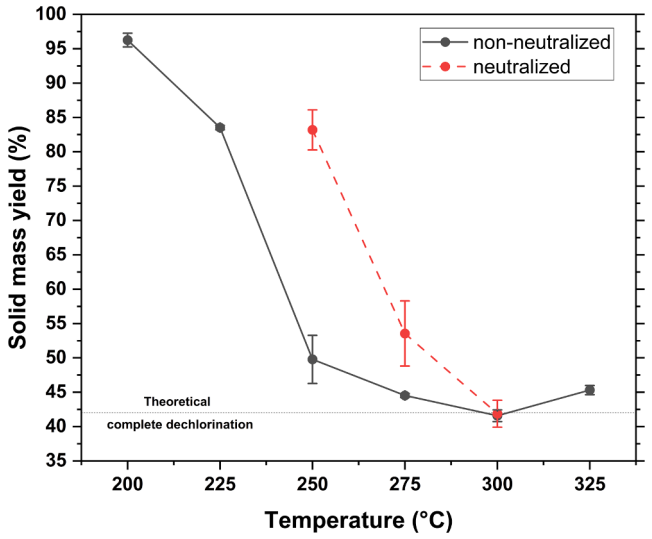

Fig. 1. Solid mass yields obtained at different temperatures. Black solid line refers to non-neutralized reactions, red dotted line refers to neutralized reactions. Reaction conditions: 1.8 g PVC, 1.81 g KOH as basic additive in the case of neutralized reaction, total mass of 9 g, 20 min. (For interpretation of the references to color in this figure legend, the reader is referred to the web version of this article.)

dechlorination was reached through the chlorine elimination pathway (Eq. (6). For this reason, complete dechlorination is expected close to 300 °C. Moreover, the color of the solid shifted from the white of the virgin PVC, to yellowish at 200 °C, brownish at 225 °C and black from 250 °C and higher. This change in color is attributed to the formation of polyenes in the solid structure, as reported in literature [33] and according to Eq. (6).

$$-(CH_2-CHCl)_n- \rightarrow -(CH=CH)_n- + n\,HCl \quad (6)$$

To enable a comparison with published literature, where the solid loadings are lower than used in this study, different concentrations of PVC were also tested. The obtained mass yields are presented in Figure S2, from which it can be observed that the impact of PVC loadings is limited. Therefore, no further investigation into PVC solid loading effects was conducted.

After the addiction of the basic additive (red line, Fig. 1), the solid residue yield was higher than without at 250 °C and 275 °C. These differences are attributed to changes in the dechlorination mechanism, which could either decrease the efficiency of dechlorination or increase the incorporation of oxygen into the solid. However, at 300 °C, the solid mass yield was equal to that of the non-neutralized reaction, representing the value that would be expected in the case of complete dechlorination via chloride elimination.

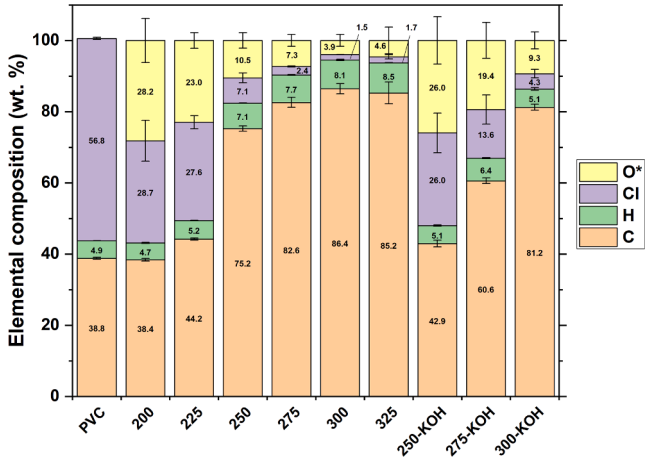

Fig. 2. Elemental composition of the solids obtained after subcritical step. Reaction conditions: 1.8 g PVC, 1.81 g KOH as basic additive in the case of neutralized reaction, total mass of 9 g, 20 min. *Oxygen has been evaluated by difference. Each sample is named after the operating temperature at which it was produced. 'KOH' was added to the name of neutralized reactions.

3.2. Elemental analysis

The elemental compositions of the solids obtained after the subcritical step are depicted in Fig. 2. Already at low reaction temperatures, the presence of chlorine diminished significantly, being replaced by oxygen. This observation highlights chlorine's susceptibility to removal within hydrothermal media and underlines the crucial role of water molecules, which are responsible for the incorporation of oxygen atoms into the solid's structure. With increasing operating temperature, the chlorine content was further reduced, reaching 1.5 wt.% at 300 °C. Conversely, the carbon content increased from 39 wt.% in PVC to approximately 85–86 wt.% beyond 300 °C, aligning with expectations of a carbonized and aromatic solid, supported by its dark appearance. Upon introducing KOH, the carbon and hydrogen contents were reduced while oxygen and chlorine contents were higher compared to the non-alkali experiments. These differences were less pronounced with increasing temperature, but they validate a deterioration in the dechlorination reaction following the introduction of the base.

Focusing on the elemental recoveries in the solids presented in Table 1, it is remarkable that carbon exhibited nearly complete retrieval across all tested temperatures. Specifically, carbon recovery spanned from 94% to 99% for non-neutralized reactions, and from 84% to 92% for neutralized reactions. Conversely, chlorine recovery decreased with increasing temperatures, resulting in notably low values: 1.1% at 300 °C without KOH and 3.1% with KOH. Consequently, the dechlorination efficiencies, which complement the chlorine recovery in the solid, were high and amounted to 98.9% and 96.9%, respectively. These outcomes are quite satisfactory due to the substantial limitation of carbon losses to other phases, most likely the aqueous phases, and the nearly complete elimination of undesired chlorine from the solid residue.

The higher heating value (HHV) of the solid samples increased with increasing temperature. For instance, the HHV progressed from 19 MJ/kg for PVC to 39 MJ/kg at 300 °C without KOH, and 33 MJ/kg with KOH (as detailed in Table 1). This enhancement is attributed to the carbon-rich structure and the relatively low presence of heteroatoms. On the other hand, at lower temperatures, the incorporation of oxygen atoms into the solid structure resulted in a decrease in calorific properties compared to virgin PVC. The fixed carbon also increased as the reaction temperature increased, moving from 8% of virgin PVC up to 54% at 300 °C, explaining the increasing carbon content of the solid.

The favorable HHV values led to an impressively high energy recovery (ER) within the solid materials. Without KOH, ER ranged from 80% to 92%, while with KOH, it ranged from 72% to 78%. Considering these findings, the dechlorination step exhibited promise by effectively eliminating nearly all chlorine, which would otherwise render the solid material unsuitable for various applications, while simultaneously preserving the majority of carbon and embedded energy from the original PVC in a solid form with a higher energy density.

To better understand the chemical mechanisms by which the dechlorination occurs, it is useful to observe the elemental molar ratios of the solids depicted as van Krevelen diagrams in Fig. 3 (A-B). In fact, two reaction mechanisms have been inferred as possible routes for the dechlorination of PVC in hydrothermal environment: elimination and substitution (Scheme 1) [28,33,34]. The elimination reaction occurs through the removal (E2 elimination) of a chloride ion from the PVC backbone, simultaneously removing an adjacent hydrogen to form a double bond [24,35,36]. Due to this elimination pathway, when a chlorine atom is removed, a hydrogen atom is also removed (pathway I

Table 1
Elemental recovery of solids after subcritical step.

	PVC	200	225	250	275	300	325	250-KOH	275-KOH	300-KOH
Carbon recovery (%)	–	95.2 ± 1.7	95.1 ± 1.0	96.5 ± 7.7	94.8 ± 2.1	94.2 ± 3.8	99.5 ± 4.9	92.0 ± 5.1	83.6 ± 8.4	87.6 ± 4.9
Chlorine recovery (%)	–	48.6 ± 10.2	40.5 ± 2.8	6.2 ± 1.6	1.9 ± 0.1	1.1 ± 0.1	1.3 ± 0.5	38.1 ± 9.5	12.8 ± 5.0	3.2 ± 1.0
Fixed carbon (wt.%)	8	13	20	47	53	54	53	11	25	29
HHV (MJ/kg)	19.4 ± 0.1	16.1 ± 0.9	19.2 ± 0.4	33.6 ± 0.6	37.1 ± 0.8	39.3 ± 0.9	39.3 ± 1.5	18.3 ± 1.2	26.6 ± 1.0	33.4 ± 1.0
ER (%)	–	79.9 ± 6.0	82.9 ± 2.6	86.4 ± 8.2	85.4 ± 3.0	85.9 ± 4.6	91.9 ± 5.5	78.4 ± 8.5	73.7 ± 9.7	72.3 ± 5.9

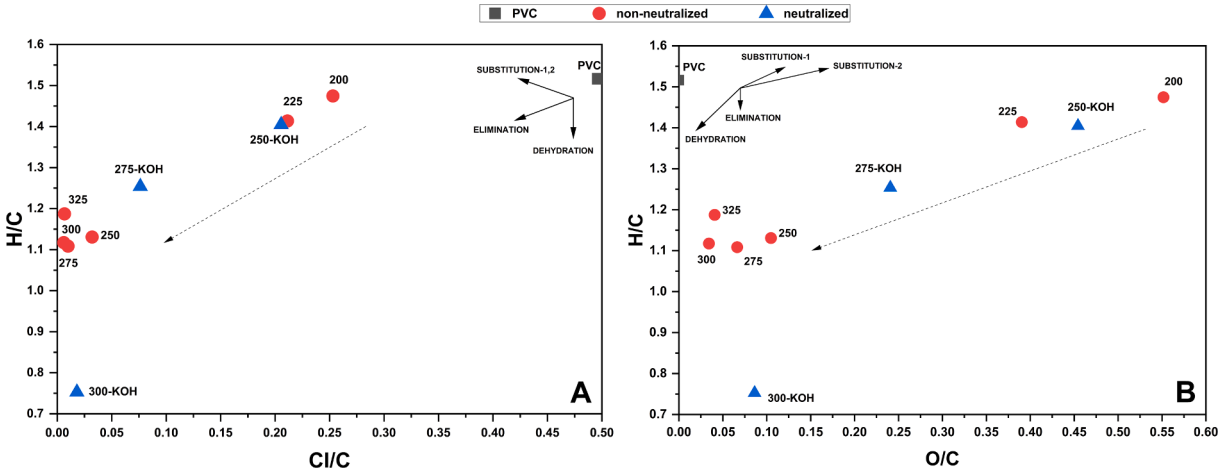

Fig. 3. Van Krevelen diagram for solids obtained after the subcritical step (A) H/C versus Cl/C and (B) H/C versus O/C.. Reaction conditions: 1.8 g PVC, 1.81 g KOH as basic additive in the case of neutralized reaction, total mass of 9 g, 20 min.

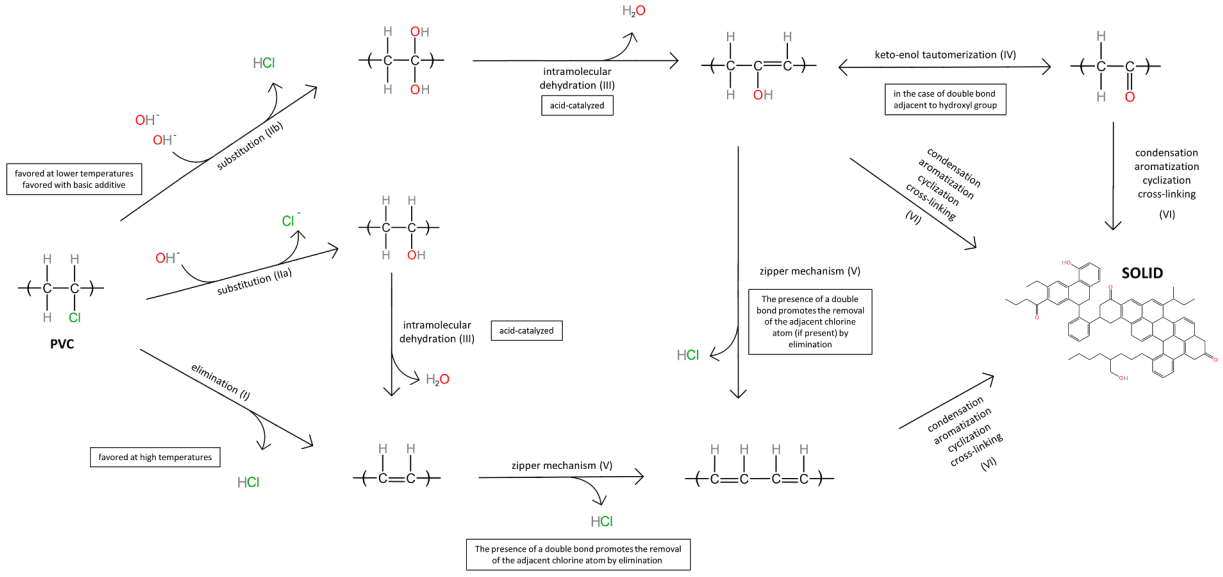

Scheme 1. Proposed reaction pathways for dechlorination of PVC in hydrothermal environment.

in Scheme 1). On the other hand, the substitution pathway involves a Sn2 nucleophilic mechanism: an OH^- ion is attracted to the carbon in the α-position, causing the release of the chloride ion [24,35,36]. With the substitution pathway, for every chlorine atom removed, one oxygen and one hydrogen atom are added to the solid (pathway IIa in Scheme 1, 'substitution-1′ in Fig. 3). In addition to this, an alternative substitution mechanism has also been observed [25,37,38], involving the simultaneous replacement of a chlorine atom and the hydrogen attached to the same carbon atom, in favor of two hydroxyl groups (pathway IIb in Scheme 1, 'substitution-2′ in Fig. 3). According to this latter mechanism, with an equal number of removed chlorine atoms, the clustered oxygen atoms result in being double.

As clearly shown in Fig. 3, at low temperatures, the primary pathway for dechlorination involves substitution. Indeed, alongside the reduction in chlorine content, there was an increase in oxygen, yielding an O/C ratio rising to 0.55 at 200 °C. In particular, the 'substitution-2′ was likely the predominant pathway, as the ratio between oxygen atoms added and the chlorine atoms removed was 2.2 and 1.5 at 200 °C and 225 °C, respectively. As temperatures rise, the O/C, H/C, and Cl/C ratios all decline. At elevated temperatures, the predominant mechanism becomes elimination. Ultimately, the resultant solids exhibited an H/C ratio close to 1, implying a predominantly aromatic structure. The Cl/C

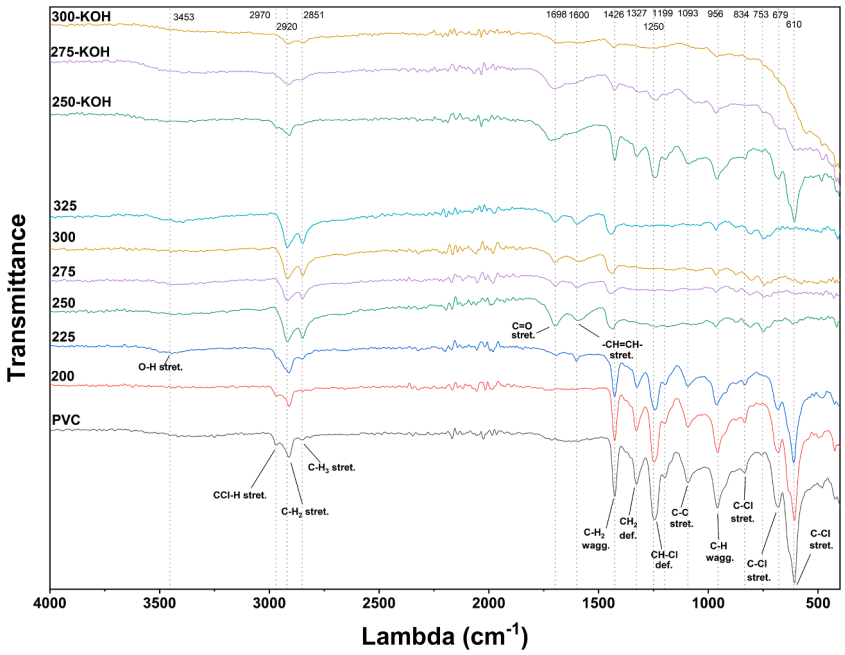

Fig. 4. ATR-FTIR of the solids obtained after the subcritical step. Reaction conditions: 1.8 g PVC, 1.81 g KOH as basic additive in the case of neutralized reaction, total mass of 9 g, 20 min.

ratio is below 0.01, and some residual oxygen was registered (O/C approximately 0.05), indicating a minor presence of the substitution reaction. In the case of addition of KOH as neutralizing additive, a lower degree of dechlorination and a higher amount of oxygen were observed at lower operating temperature. Interestingly, at 300 °C, O/C and Cl/C ratios similar to the non-neutralized reaction were obtained, whereas the H/C was consistently lower (0.75). This suggests a difference in the dechlorination mechanism, which will be deepened below (3.5 *Kinetic evaluation and dechlorination mechanism*). To summarize, from Fig. 3 it is evident that to achieve nearly complete chlorine elimination, the primary mechanism required is elimination.

3.3. FTIR

Fig. 4 presents the ATR-FTIR spectra of PVC and solids. Functional groups were identified based on values reported in the literature [39,40]. Looking at the virgin PVC spectrum, various peaks are associated with the presence of chlorine within the structure, namely at 1250, 834, 679 and 610 cm^{-1}. The last one is linked to the stretching of the C-Cl bond and is the most intense peak. At low temperatures (200 °C and 250 °C), the resulting spectra closely resembled that of virgin PVC. Despite the removal of chlorine from the structure, it appears that the overall structure did not change significantly. However, as indicated by the elemental analysis, substitution was likely the main mechanism occurring at low temperatures, leading to an increase in the oxygen content of the solids. Due to this reason, the presence of peaks associated with bonded oxygen would be expected, particularly for the solid obtained at 200 °C, given that oxygen accounted for 28% of its total mass. However, in the region around 3300–3400 cm^{-1}, where the stretching of the O–H bond absorbs, the signal intensity was low. This low signal intensity can be attributed, in part, to the sharpness of the peaks at low wavelengths, which tends to overshadow broader peaks like that of the hydroxyl group. Additionally, since PVA (polyvinyl alcohol) is prone to undergo cross-linking when exposed to heat [41], it is plausible that during the drying phase (overnight at 105 °C), some hydroxyl groups in the chain underwent cross-linking, diminishing their vibration and, consequently, their intensity in the FTIR spectrum. Moreover, Yao et al. also did not register a significant difference in intensity at 3300 cm^{-1} between PVC and the solid obtained after hydrothermal treatment of PVC at 200 °C for 60 min, even though the latter contained 13 wt.% of oxygen [37]. At 250 °C, the signal at 610 cm^{-1} was weak and above 250 °C it became invisible, suggesting that FTIR is not sensitive to chlorine concentrations below 5 wt.%. On the other hand, signals at 1698 and 1600 cm^{-1} emerged at temperatures above 250 °C. The former is associated with C=O stretching, likely of an aromatic or unsaturated nature, due to its lower frequency (<1700 cm^{-1}) [42]. The formation of C=O could result from substitution of chlorine with two hydroxyl groups (pathway IIb in Scheme 1), their intramolecular dehydration (pathway III in Scheme 1) and subsequent keto-enol tautomerization (pathway IV in Scheme 1) [25,37]. The peak at 1600 cm^{-1} is attributed to the aromatic C=C bond, and its presence, coupled with the H/C ratio nearing 1, supports the formation of an aromatic structure as the reaction temperature rises. However, no peaks were visible at wavelengths above 3000 cm^{-1}, the region of the spectrum associated to the presence of double bonds. Some char and biochar standards were tested (Figure S3) as references, and in both cases no signals were recorded above 3000 cm^{-1}. This confirms that even though double bonds may be present, their corresponding signals are not detected in the spectra.

In the case of KOH addition, at 250 °C, the peaks associated with C-Cl (1250 and 610 cm^{-1}) remain the most intense; at 275 °C further decrease, and at 300 °C they are no longer visible. This is consistent with the chlorine content estimated by μ-XRF. As seen without KOH, at 250 °C the peak associated to C=O emerges, along with a peak shoulder for the C=C bond. Although there was a baseline drift towards lower wavelengths for the solid obtained at 300 °C with KOH, the peaks resembled those observed without the addition of KOH.

3.4. TGA and Pyro-GC–MS

TGA and DTGs for the virgin PVC and for the solids obtained after the first hydrothermal step are reported in Fig. 5. Two main peaks were discernible: the first was centered at 290–311 °C, while the second peak at 446–465 °C. As widely acknowledged, the initial weight loss attributed to dechlorination in the case of PVC during dry and inert conditions (pyrolysis-like) is characterized by the removal of chlorine as HCl [43]. As registered in hydrothermal environment, during TGA, the dechlorination reaction started at around 250 °C and led to a mass decrease in PVC of 63% by 380 °C. As the temperature at which the solid material

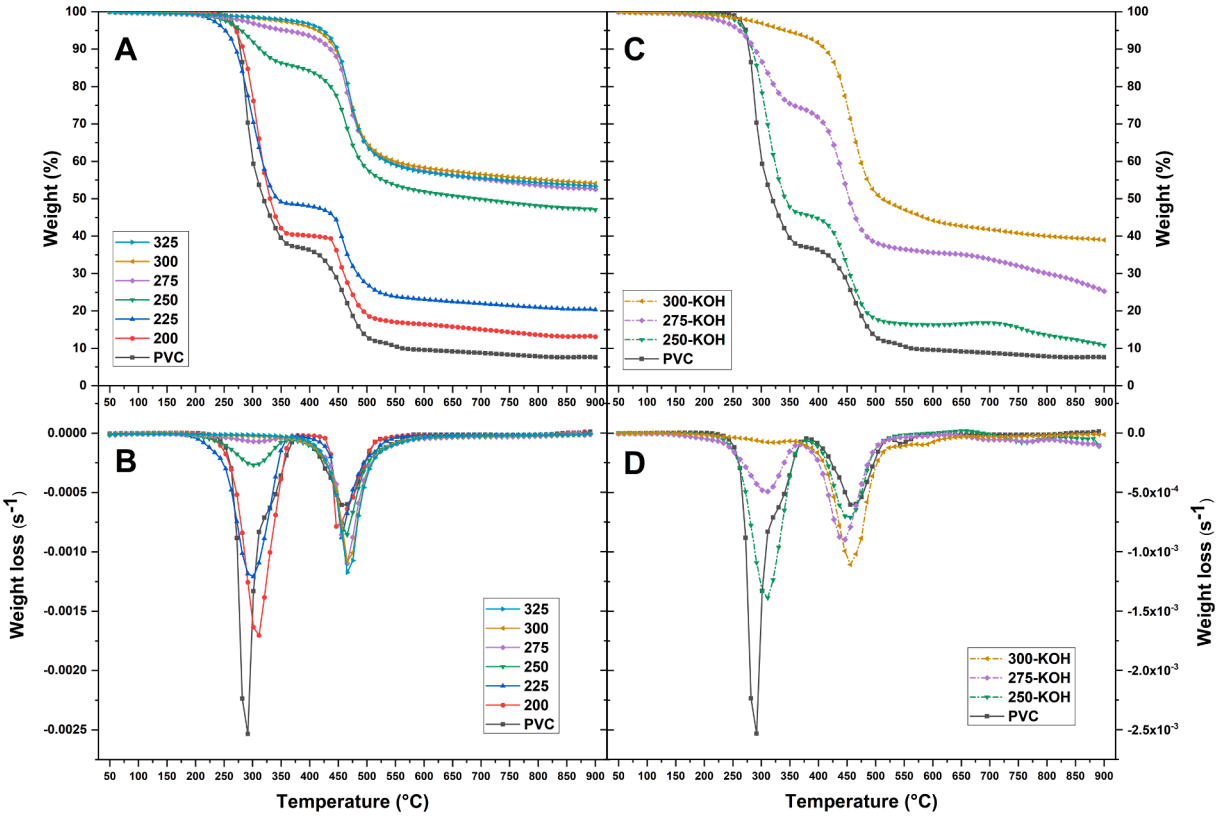

Fig. 5. TGAs and DTGs of virgin PVC and solids obtained after the subcritical step. (A) TGA and (B) DTG of solid produced through non– neutralized reaction. (C) TGA and (D) DTG of solid produced through neutralized reaction. Reaction conditions: 1.8 g PVC, 1.81 g KOH as basic additive in the case of neutralized reaction, total mass of 9 g, 20 min.

Table 2
Mass losses calculated from DTG. *The normalized mass loss is calculated according to Eq. (7).

	PVC	200	225	250	275	300	325	250-KOH	275-KOH	300-KOH
1st mass loss (204°C-379°C)	62.8%	59.5%	50.7%	13.9%	4.8%	2.6%	1.9%	53.9%	24.7%	4.9%
2nd mass loss (379°C-550°C)	25.4%	22.8%	23.6%	30.0%	33.2%	35.0%	36.5%	29.2%	37.3%	40.5%
Normalized* 2nd mass loss (379°C-550°C)	25.4%	21.9%	19.7%	14.9%	14.8%	14.8%	16.6%	24.3%	20.0%	22.3%

was generated increased, the reduction in mass yield associated with the dechlorination reaction decreased, as detailed in Table 2. This is coherent with μ-XRF results. Moreover, as described above, the residual chlorine was increased in the case of the neutralized reactions (depicted in Fig. 5C-D), resulting in an increased mass loss associated with the first peak with respect to that of non-neutralized reactions (Fig. 5A-B) at the same operating temperature.

At temperatures above 380 °C, the samples experienced a second mass loss, which is commonly associated with the breakdown of the structure formed after dechlorination [43,44]. The reduction in mass at this stage was more pronounced at higher operating temperatures (Table 2, Fig. 5B-D). However, as depicted in Fig. 1, elevated operating temperatures led to a greater weight reduction. In order to establish a connection between the loss of mass and the initial quantity of PVC, we also calculated the TGA mass loss normalized by the solid yield achieved after the subcritical process (Eq. (7). As detailed in Table 2, the normalized data showed an opposite pattern, indicating that, in comparison to the solid formed after the initial PVC dechlorination peak in TGA, the hydrothermal-derived solids are less susceptible to decomposition through pyrolysis. This suggests that the first hydrothermal step might have induced chemical modifications in the PVC structure, differentiating it from the pyrolysis behavior of untreated PVC at 380 °C and beyond. Moreover, the addition of the basic additive increased the normalized mass loss (Table 2, Fig. 5D), suggesting that the solid structure formed during the neutralized dechlorination was more susceptible to further conversion.

$$Normalized TGA mass loss\left(\frac{g lost during TGA}{g starting PVC}\right) = TGA mass loss\left(\frac{g lost during TGA}{g dechlorinated solid}\right)\cdot solid mass yield\left(\frac{g dechlorinated solid}{g starting PVC}\right) \quad (7)$$

Py-GC–MS was conducted at a pyrolysis temperature of 600 °C using the solid obtained after the subcritical step, aiming at a better understanding of its structure. The semiquantitative analysis of the volatile compounds is reported in Fig. 6. It is evident that a substantial quantity of aliphatic hydrocarbons (including linear/cyclic alkanes, linear/cyclic monounsaturated alkenes and dienes/trienes) was present. This is noteworthy considering that Py-GC–MS converts many aliphatic hydrocarbons into aromatics during pyrolysis [45,46], and that the amount of aliphatic hydrocarbons observed in this work was higher than typical values obtained from biochar [47].

Py-GC–MS of virgin PVC results in the formation of low alkanes and high amount of aromatics [48]. This is explained by the fact that the pyrolysis of PVC appears to proceed through free-radical reactions that lead to the release of chlorine, forming radicals that subsequently convert into monocyclic aromatics and PAHs (polycyclic aromatic

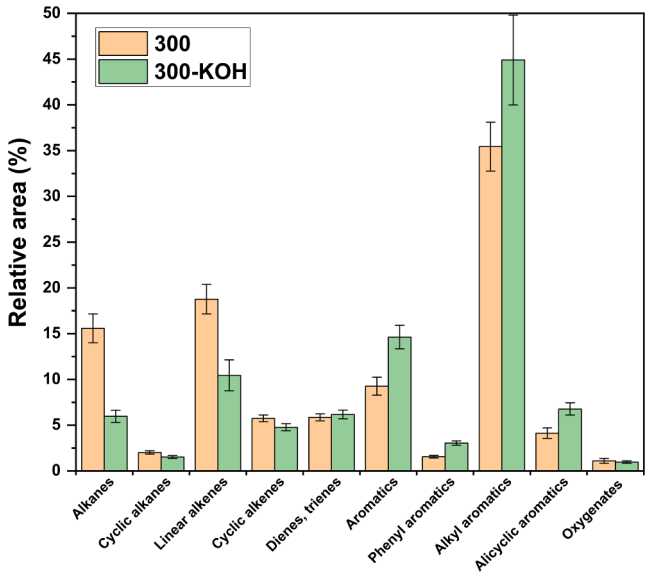

Fig. 6. Products distribution from Py-GC–MS at the pyrolysis temperature of 600 °C of the solids produced in subcritical water at 300 °C without KOH (orange) and with KOH (green). Subdivision was performed based on substitution groups. 'Phenyl,' 'alkyl,' and 'alicyclic' indicate the nature of the substituents. As dienes and trienes were accounted both aliphatic and alicyclic structures. Data are expressed as relative area with respect to all identified peaks. (For interpretation of the references to color in this figure legend, the reader is referred to the web version of this article.)

hydrocarbons) [48]. Interestingly, literature reports that long-chain aliphatics (ranging from C7 to C22) were almost absent in the Py-GC–MS of virgin PVC [48]. In contrast, we observed after Py-GC–MS analysis of the dechlorinated samples, long-chain aliphatic hydrocarbons accounting for 11% and 24% of the total integrated area in solids obtained with and without KOH, respectively. Therefore, it is probable that these saturated hydrocarbons found in the dechlorinated solid originate from the degradation of extended aliphatic chains already present in the solid structure. However, it is essential to stress that during Py-GC–MS, as indicated by TGA in Fig. 5, only 42% (without KOH) and 58% (with KOH) of the solids were converted into volatiles and, therefore, were subject to analysis. For this reason, it is reasonable to assume that the remaining portion is composed of a more heavily condensed, charred phase, which would explain the low molar H/C ratio of the two solid.

The addition of KOH during the subcritical step led to a higher share of aromatics at the expense of aliphatic hydrocarbons. This shift in product distribution made it resemble pure PVC more closely. This change can be related to a lower abundance of aliphatic branches or to a higher amount of unsaturation within the solid. The latter hypothesis is more likely as the H/C ratio was lower than that of the solid obtained without adding KOH.

The signal associated with HCl was too weak to be identified, confirming the low level of chlorine remaining in the solids. Additionally, the only chlorine-containing compound detected was chlorobenzene, but it was found with negligible intensities. This finding suggests the potential to obtain a chlorine-free product after pyrolysis of the dechlorinated solid. However, it is worth noting that even in the Py-GC–MS analysis of virgin PVC, no chlorinated compounds were observed at pyrolysis temperatures exceeding 600 °C [48], implying a limited sensitivity of Py-GC–MS in detecting such compounds. The intensity of oxygen-containing molecules was also very low, comprising approximately 1% of the overall identified area.

3.5. Kinetic evaluation and dechlorination mechanism

Fig. 7A depicts the points obtained by the DSC using the Kissinger method, as described in the Material and Methods section. These data were subjected to linear interpolation using Eq. (5), allowing for the calculation of apparent activation energies and pre-exponential factors, which are summarized in Table 3. For the hydrothermal dechlorination of PVC without neutralization, the apparent activation energy was determined to be 185.9 ± 6.8 kJ/mol, and the pre-exponential factor was found to be $1.42{\cdot}10^{17}$ min^{-1}. The calculated activation energy value aligns closely with the activation energies of 187 kJ/mol and 190 kJ/mol reported for hydrothermal dechlorination of PVC powder by Hashimoto et al. [49] and Li et al. [50], respectively. Notably, this

Table 3
Kinetic parameters for neutralized and non-neutralized dechlorination of PVC in subcritical water.

		non-neutralized	neutralized
E_a, activation energy (kJ/mol)	Mean value	185.9	119.8
	Confidence interval	179.1–192.7	112.8–126.8
k_∞, pre-exponential factor (min^{-1})	Mean value	$1.42{\cdot}10^{17}$	$6.14{\cdot}10^{10}$
	Confidence interval	$3.11{\cdot}10^{16}$–$6.45{\cdot}10^{17}$	$1.26{\cdot}10^{10}$–$2.98{\cdot}10^{11}$

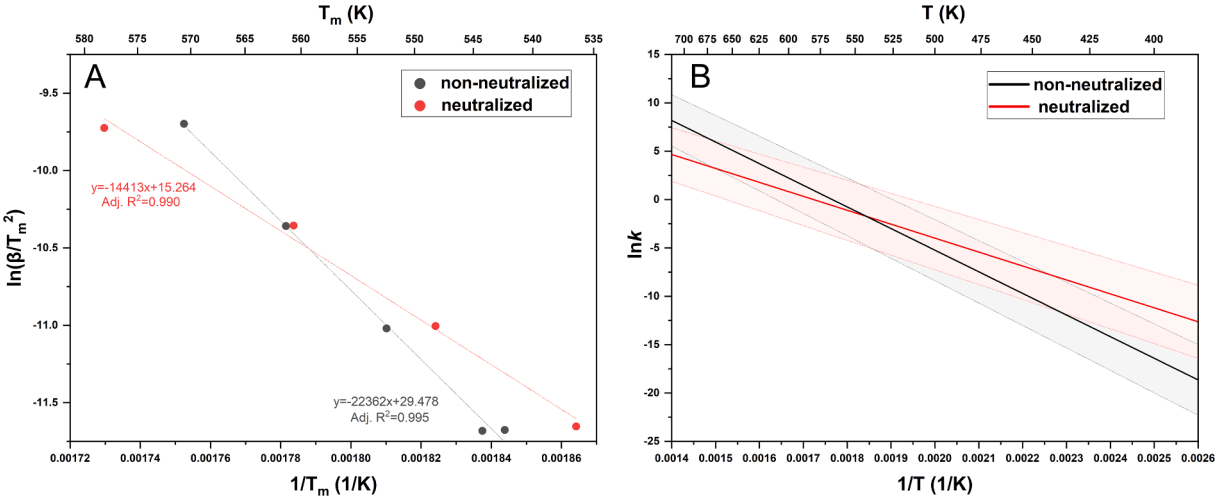

Fig. 7. (A) linear interpolation of data obtained after DSC by KAS method, (B) lnk versus 1/T for the dechlorination reaction. Shadows represent the confidence interval.

agreement is significant since our study is the first to employ the Kissinger method for evaluating these hydrothermal kinetic parameters. The values reported for the pre-exponential factor by Hashimoto et al. and Li et al. were $5.23{\cdot}10^{16}$ min^{-1} and $1.86{\cdot}10^{16}$ min^{-1} [49,50]. The former value falls within the confidence interval of our findings, while the latter is slightly lower. Based on these apparent activation energy values, it can be inferred that the dechlorination reaction is primarily controlled by chemical reactions and not by mass transfer limitations [35]. Additionally, prior literature has indicated that the dechlorination process adheres to first-order kinetic behavior [35,50–52].

In the case of addition of KOH, the apparent activation energy decreased from 185.9 ± 6.8 kJ/mol to 119.8 ± 7.0 kJ/mol and the pre-exponential factor decreased from $1.42{\cdot}10^{17}$ min^{-1} to $6.14{\cdot}10^{10}$ min^{-1}. Based on these results, it can be inferred that the addition of KOH kinetically favors the dechlorination reaction at lower temperatures while becoming unfavored at higher temperatures. This is confirmed by Fig. 7B, which shows the plot of the reaction velocity of dechlorination (ln*k*) versus the inverse of the reaction temperature (1/T). It can be observed that below ca. 270 °C the neutralized reaction has higher dechlorination rates while at higher temperatures the non-neutralized reaction favors the dechlorination rate. Similar kinetic results were observed also in the literature. Hashimoto et al. observed a decrease in both activation energy (120 vs 187 kJ/mol) and pre-exponential factor ($3.0{\cdot}10^{11}$ vs $5.2{\cdot}10^{16}$ min^{-1}) when a 0.6 M solution of ammonia was used instead of water for hydrothermal dechlorination of PVC powder [49]. Shin et al. registered apparent activation energies within 92–146 kJ/mol in 1–7 M NaOH solution for flexible PVC pellets [51]. From the same feedstock, the same group evaluated the activation energy as low as 89–103 kJ/mol using a 1.0 M NaOH in ethylene glycol instead of water as solvent [35]. However, unlike literature, in this work the dechlorination efficiency decreased at low temperatures if KOH was added in the reactor.

As documented in various sources [23,35,53], it was noted that incorporating a basic additive during the dechlorination of PVC increases the presence of hydroxyl ions (OH^-). These ions play a role in promoting the substitution mechanism (pathway IIa and pathway IIb in Scheme 1). By employing the Kissinger method via DSC analysis, the determined apparent activation energy in the case of neutralized reactions is likely associated with this pathway. Therefore, in addition to its neutralization role, KOH acts as a catalyst. This assumption is supported by the fact that at 250 °C the O/C molar ratio was increased with addition of KOH (Fig. 3). Nevertheless, achieving a high degree of chlorine removal efficiency may require the utilization of the elimination mechanism (pathway I in Scheme 1), as discussed above (3.2 *Elemental analysis*). This mechanism is associated with the activation energy of 186 kJ/mol and is not only thermally favored but also self-propagating due to the 'zipper mechanism' (pathway V in Scheme 1): the formation of a double bond following the removal of a HCl molecule from the PVC structure triggers the adjacent chlorine atom's activation, facilitating the spread of the chlorine removal process throughout the PVC structure [54–56].

By giving preference to the substitution of chloride ions with hydroxyl ions, the effectiveness of the 'zipper mechanism' is hindered. This is further exacerbated by the high amount of KOH introduced in this study, which elevates the solution's pH to a highly basic level. Consequently, this high basicity could deter the dehydration reaction (pathway III in Scheme 1), as it is known to be acid-catalyzed [24,57]. As a result, the hydroxyl groups produced after the substitution process are unable to transform into the polyene structure, ultimately limiting the effectiveness of chlorine removal in the presence of KOH. This theory may also elucidate why existing literature indicates that the addition of basic additives initially enhances chlorine removal but eventually reaches a point where further increases in alkali concentration leads to diminishing returns [27,51]. Indeed, a moderate amount of alkali can aid the dechlorination by substitution, resulting in the formation of a carbon backbone with hydroxyl groups. The basicity of the starting solution is limited and as the reaction proceeds, the aqueous phase ends up being acidic due to the high amount of chlorine released. This shift in conditions could facilitate intramolecular dehydration, forming the polyene structure which can then initiate the 'zipper mechanism'. The polyenes are prone to instability and easily tend to react. They engage in intramolecular reactions, leading to cyclization, aromatization, polymerization, and cross-linking [32,43,58,59]. Consequently, the resulting solid likely comprises a substantial quantity of polyaromatic structures, along with aliphatic branches and hydrogenated aromatics (pathway VI in Scheme 1).

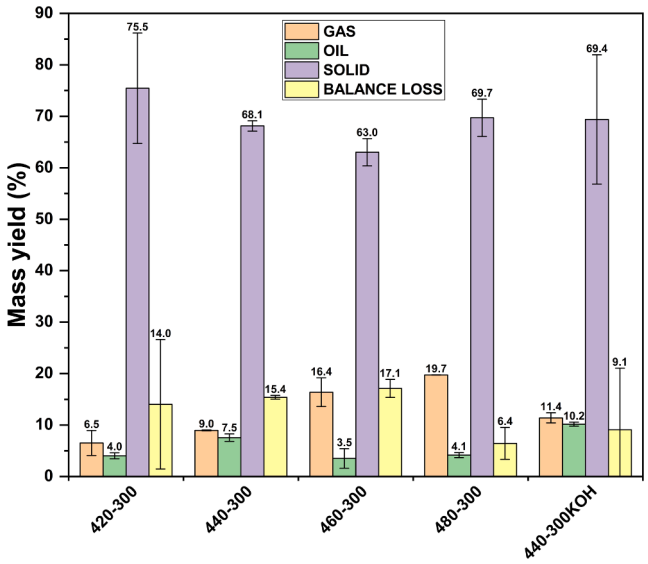

Fig. 8. Mass yields obtained after the supercritical step of the solids obtained from the subcritical step. Reaction conditions: 0.832–1.084 g of dechlorinated solid (depending on the temperature), solid/water ratio of 1/2, 60 min, 225 bar. The first number in the experiment denotes the temperature of the supercritical step, while the second number pertains to the sample used as the feedstock for the supercritical step.

3.6. *Supercritical step*

Fig. 8 presents the mass yields of the products obtained after supercritical HTL at varying temperatures. As the reaction temperature increases, the amount of produced gas also rises from 6.5% to 19.7%. This trend was anticipated, considering that gas production is known to escalate with reaction temperature in hydrothermal liquefaction [18,60]. The gas composition is predominantly composed of aliphatic compounds, as observed by Takeshita et al. from the hydrothermal decomposition of PVC at 400 °C [32].

The oil formation after the supercritical step was rather limited. The maximum production was registered at 440 °C, yielding 7.5 wt.% and 10.2 wt.% using the solid produced in the absence and presence of KOH, respectively. The sum of oil and gas was in fact increasing with increasing temperature, suggesting that higher temperatures led to degradation of the oil phase into gaseous hydrocarbons. Moreover, a portion of the oil was lost after evaporation of the extraction solvent, as shown in Figure S1. This hypothesis was confirmed by the fact that the amount of carbon missed in the aqueous phase was quantified as 0.1% of the carbon present in the dechlorinated solid used as the feedstock for the supercritical step. It is hence reasonable to assume that the missing mass (yellow columns in Fig. 8) was composed of low-boiling oil compounds. For this reason, the composition of the oil was studied prior to drying; the results are depicted in Fig. 9, along with the results obtained from Py-GC–MS, in order to highlight the differences between fast pyrolysis and supercritical HTL as the processing step.

The products obtained after supercritical HTL at 440 °C were mainly

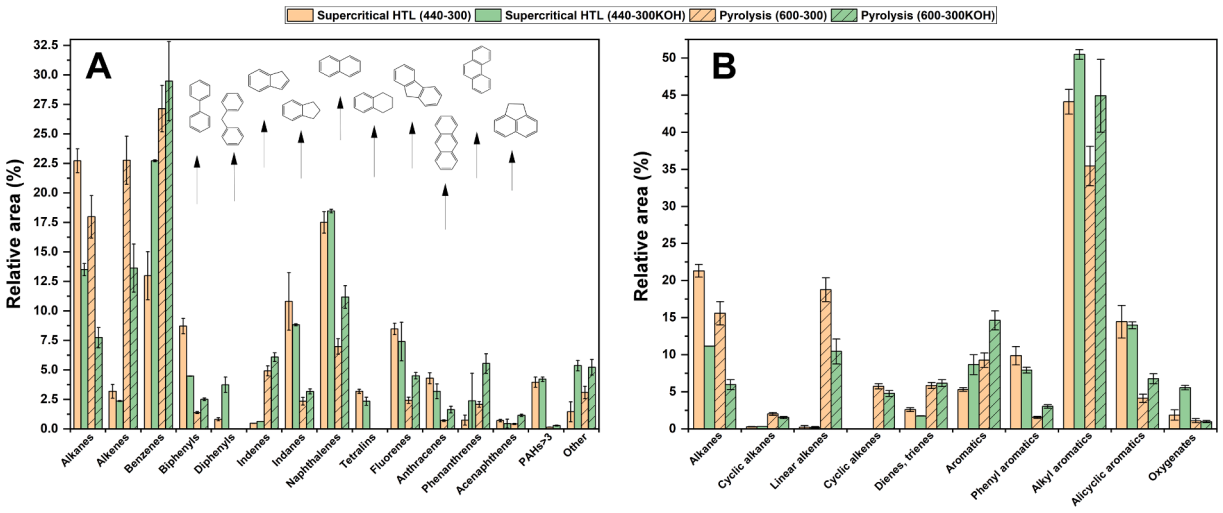

Fig. 9. GC–MS chromatograms of the oil obtained after the supercritical step at 440 °C (bars without pattern) and chromatogram obtained from Py-GC–MS for comparison purposes (hatched bars). The compounds in the chromatograms are categorized in two ways: (A) based on their aromatic structure or (B) based on their functionalities. 'Phenyl,' 'alkyl,' and 'alicyclic' indicate the nature of the substituent groups. Orange bars refer to the oil obtained using as feedstock the solid produced at 300 °C without KOH; green bars refer to the oil obtained using as feedstock the solid produced at 300 °C with KOH. Data are expressed as relative area with respect to all identified peaks. (For interpretation of the references to color in this figure legend, the reader is referred to the web version of this article.)

aromatics. In particular, PAHs largely outnumbered other compounds, accounting for ca. 50% of the overall area of the chromatograms. Among these, the naphthalene derivatives were the most prevalent, with the remaining PAHs following in sequence from lightest to heaviest (Fig. 9A). Moreover, some partially hydrogenated derivatives of PAHs ('alicyclic aromatics' in Fig. 9B) were also present, in particular indanes and tetralins (Fig. 9A). Other than these, the most abundant molecules were alkanes and benzene derivatives. Interestingly, the distribution between these two families was the biggest difference observable between the use of solids obtained with KOH and without KOH. Without KOH, a higher share of alkanes and a lower production of benzene derivatives was registered with respect to the addition of KOH. As previously discussed for fast pyrolysis, this may be symptomatic of a higher quantity of saturated aliphatic chains in the absence of basic additive.

Although a consistent amount of alkanes was also registered after supercritical HTL, few alkenes were identified. This is interesting, as more alkenes than alkanes resulted after fast pyrolysis. Moreover, with respect to supercritical HTL, fast pyrolysis favored the production of monoaromatics (benzenes) at the expenses of PAHs, and increased the presence of unsubstituted aromatics at the expenses of alkylated and alicyclic aromatics (Fig. 9B). These observations suggest that pyrolysis results in higher cracking of the dechlorinated solid, increasing dealkylation and unsaturation of the product.

After supercritical HTL, the amount of chlorinated compounds identified in the chromatograms was very low, amounting to 0.34 ± 0.30% and to 0.74 ± 0.35% of the overall identified area, in the case of 440–300 and 440-300KOH, respectively. This is an improvement with respect to the production of oil directly from PVC, as many chlorinated compounds were found in the oil [54]. On the other hand, the presence of oxygen was not irrelevant. Indeed, 4.4 ± 0.7% and 10.0 ± 1.0% of the overall identified area was constituted by oxygen-containing molecules, in the case of 440–300 and 440-300KOH, respectively (Fig. 9B). The higher amount of oxygenated compounds compared to fast pyrolysis suggests the active role of water molecules during the supercritical reaction.

After the supercritical step, most of the solid remained as such. In fact, the solid yield ranged between 63 and 76%, corresponding to a conversion of 24–37%. Interestingly, the conversion of the solid material did not consistently rise with temperature; instead, it reached a peak at 440 °C. The introduction of KOH during the subcritical phase did not affect the solid conversion, but slightly increased the production of oil and gas. With respect to supercritical HTL, with fast pyrolysis at 600 °C (Fig. 5), solid conversion would be increased from 31 to 56% and from 32 to 42%, in the case of dechlorinated solid obtained at 300 °C with and without KOH, respectively.

Similar to the mass yield, the carbon yield within the solid phase ranged between 64% and 79% after the supercritical step (as outlined in Table 4). The carbon content remained similar to that registered prior to the supercritical step (around 90%). On the other hand, hydrogen decreased as the operating temperature increased. Consequently, the H/C molar ratio dropped from a starting 1.1 after the subcritical step to 0.29 after the supercritical step at 480 °C. The solid hence moved towards a heavier anthracite-like structure, as confirmed also by the higher fixed carbon. Furthermore, the chlorine content diminished even further, reaching approximately 1 wt.%, while the O/C ratio experienced a slight increase, confirming the incorporation of oxygen from

Table 4
Elemental compositions, carbon recovery and HHV for solids obtained after the supercritical step.

		420–300	440–300	460–300	480–300	440-300KOH
Elemental composition (wt.%)	**C**	90.3 ± 0.3	86.5 ± 5.8	87.7 ± 1.9	86.4 ± 1.8	92.2 ± 2.4
	H	6.1 ± 0.3	3.1 ± 0.2	2.5 ± 0.2	2.1 ± 0.2	3.9 ± 0.2
	Cl	1.0 ± 0.3	0.7 ± 0.3	1.1 ± 0.1	1.0 ± 0.1	1.1 ± 0.1
	O	2.6 ± 0.9	9.7 ± 6.2	8.7 ± 2.2	10.6 ± 2.1	2.7 ± 2.5
Elemental molar ratio	**H/C**	0.81 ± 0.05	0.42 ± 0.05	0.34 ± 0.04	0.29 ± 0.04	0.51 ± 0.04
	Cl/C	0.004 ± 0.001	0.003 ± 0.001	0.004 ± 0.001	0.004 ± 0.000	0.004 ± 0.001
	O/C	0.02 ± 0.01	0.08 ± 0.06	0.07 ± 0.02	0.09 ± 0.02	0.02 ± 0.02
Carbon recovery in solid (%)		78.8 ± 12.7	68.2 ± 6.7	64.0 ± 5.1	69.7 ± 6.2	78.9 ± 17.3
Fixed carbon (wt.%)		66	67	90	85	69
HHV (MJ/kg)		38.5 ± 0.4	32.8 ± 1.6	32.7 ± 0.7	31.5 ± 0.7	36.5 ± 0.8

water. Due to the reduced hydrogen content and increased oxygen content, the energy content of the solid material decreased after the supercritical step.

3.7. Perspectives

Overall, the double-stage hydrothermal process suggested showed to be an interesting way of valorizing PVC waste. The subcritical stage it was possible to remove 99% of the chlorine present in the virgin PVC under the form of HCl. The produced HCl solution could then be used as reagent for virgin PVC. Simultaneously, nearly all the carbon remains within the solid. This selective removal of chlorine leads to an increase in the heating value of the remaining solid material, thereby enabling substantial energy recovery. It is hence possible to generate a solid that is both denser in energy content and nearly devoid of chlorine, enabling its easier use as feedstock for subsequent technologies.

Including the supercritical stage, it was possible to reduce the solid to 29% of the starting PVC mass, containing approximately 64% of the carbon content of PVC. Simultaneously, gaseous and liquid hydrocarbons were produced, constituting 30% of the carbon content of the initial PVC. It is assumed that the missing carbon in the supercritical step is constituted by light oil rich in aromatic compounds, as no carbon was found in the aqueous phase. The solid phase could then be energy valorized while the oil can be used as source of aromatics for chemicals.

Lastly, although the results obtained in this work by adding the neutralizing agent (KOH) did not show major differences with the non-neutralized case, the use of basic additives could be helpful from a technical perspective. Indeed, dechlorination reaction showed high corrosivity issues [24] that were also registered in this work, given the very high solid loading used (20 wt.%) and the use of stainless steel as reactor material. Adding the basic additive already in the dechlorination reactor, might allow for an in-situ neutralization that would preserve the reactor from corrosion. In this study, such improvements were not observed. However, further investigations into the use of KOH could allow for a better understanding and provide a solution to the problem.

4. Conclusions

This experimental study presented a two-stage hydrothermal processing for the energy valorization of PVC waste. In the first subcritical stage, by operating at 300 °C for 20 min, it was possible to achieve a remarkable 99% removal of chlorine, while retaining 94% of the carbon content in the solid produced. The addition of KOH, as neutralizing additive, during the subcritical stage proved to catalytically favor the substitution mechanism as a dechlorination pathway, albeit hindering high dechlorination efficiency at low operating temperatures. The catalytic activity was confirmed by a reduction in the apparent activation energy (from 186 to 120 kJ/mol) by addition of KOH. At 300 °C, the impact of KOH on performance was less pronounced. Through various analytical techniques (CHNS, Py-GC–MS, FTIR and TGA), the resulting solid was observed to consist mainly of a condensed aromatic structure with aliphatic branches. Following the supercritical stage, the residual solid underwent a reduction to 29% of the mass of the initial PVC. Concurrently, liquid and gaseous hydrocarbons were produced, accounting to 30 % of the carbon present in the PVC. Using supercritical HTL for valorizing the dechlorinated solid lead to the production of an oil phase containing a higher share of PAHs and alkylated aromatics and a higher degree of saturation, with respect to pyrolysis products. Overall, the subcritical stage demonstrated its efficiency in producing a nearly chlorine-free solid material with a higher energy density than that of PVC. The dechlorinated solid could then be further processed using other technologies. To implement this on an industrial scale, further advancements are required to address issues related to corrosion, and the incorporation of additives could be a potential means of addressing it.

CRediT authorship contribution statement

Edoardo Tito: Writing – original draft, Visualization, Methodology, Investigation, Formal analysis. **Juliano Souza dos Passos:** Writing – review & editing, Investigation, Formal analysis, Conceptualization. **Alessandro Girolamo Rombolà:** Writing – review & editing, Formal analysis, Data curation. **Cristian Torri:** Writing – review & editing, Formal analysis. **Samir Bensaid:** Supervision. **Raffaele Pirone:** Supervision. **Patrick Biller:** Writing – review & editing, Supervision, Resources, Project administration, Methodology, Funding acquisition, Conceptualization.

Declaration of competing interest

The authors declare that they have no known competing financial interests or personal relationships that could have appeared to influence the work reported in this paper. This research was funded by the Independent Research Foundation Denmark project CatPol: Catalytic depolymerization of synthetic polymers, grant number 1032–00263B.

Data availability

Data will be made available on request.

Appendix A. Supplementary data

Supplementary data to this article can be found online at https://doi.org/10.1016/j.enconman.2024.118228.

References

[1] Shanmugam V, Das O, Neisiany RE, Babu K, Singh S, Hedenqvist MS, et al. Polymer recycling in additive manufacturing: An opportunity for the circular economy. Mater Circ Econ 2020;2. https://doi.org/10.1007/s42824-020-00012-0.
[2] Geyer R, Jambeck JR, Law KL. Production, use, and fate of all plastics ever made. Sci Adv 2017;3:3–8. https://doi.org/10.1126/sciadv.1700782.
[3] Li H, Aguirre-Villegas HA, Allen RD, Bai X, Benson CH, Beckham GT, et al. Expanding plastics recycling technologies: chemical aspects, technology status and challenges. Green Chem 2022;24:8899–9002. https://doi.org/10.1039/D2GC02588D.
[4] Van Geem KM. Plastic waste recycling is gaining momentum. Science (80-) 2023;381:607–8. https://doi.org/10.1126/science.adj2807.
[5] Garcia-Gutierrez P, Amadei AM, Klenert D, Nessi S, Tonini D, Tosches D, Ardente F, Saveyn H. Environmental and economic assessment of plastic waste recycling. 2023. https://doi.org/10.2760/0472. ISSN 1831-9424. ISBN 978-92-76-99528-9.
[6] Plastics-The Facts 2022, 2020.
[7] Edo C, Fernández-Piñas F, Rosal R. Microplastics identification and quantification in the composted Organic Fraction of Municipal Solid Waste. Sci Total Environ 2022;813:151902. https://doi.org/10.1016/j.scitotenv.2021.151902.
[8] Schwarzböck T, Van Eygen E, Rechberger H, Fellner J. Determining the amount of waste plastics in the feed of Austrian waste-to-energy facilities. Waste Manag Res 2017;35:207–16. https://doi.org/10.1177/0734242X16660372.
[9] Seshasayee MS, Savage PE. Oil from plastic via hydrothermal liquefaction: Production and characterization. Appl Energy 2020;278:115673. https://doi.org/10.1016/j.apenergy.2020.115673.
[10] Zeller M, Netsch N, Richter F, Leibold H, Stapf D. Chemical recycling of mixed plastic wastes by pyrolysis – pilot scale investigations. Chem-Ing-Tech 2021;93:1763–70. https://doi.org/10.1002/cite.202100102.
[11] Mumtaz H, Sobek S, Werle S, Sajdak M, Muzyka R. Hydrothermal treatment of plastic waste within a circular economy perspective. Sustain Chem Pharm 2023;32:100991. https://doi.org/10.1016/j.scp.2023.100991.
[12] Li N, Liu H, Cheng Z, Yan B, Chen G, Wang S. Conversion of plastic waste into fuels: A critical review. J Hazard Mater 2022;424:127460. https://doi.org/10.1016/j.jhazmat.2021.127460.
[13] Yang R-X, Jan K, Chen C, Chen W-T, Wu K-C-W. Thermochemical conversion of plastic waste into fuels, chemicals, and value-added materials: A critical review and outlooks. ChemSusChem 2022;15. https://doi.org/10.1002/cssc.202200171.
[14] Anuar Sharuddin SD, Abnisa F, Wan Daud WMA, Aroua MK. A review on pyrolysis of plastic wastes. Energy Convers Manag 2016;115:308–26. https://doi.org/10.1016/j.enconman.2016.02.037.
[15] Roosen M, Mys N, Kusenberg M, Billen P, Dumoulin A, Dewulf J, et al. Detailed analysis of the composition of selected plastic packaging waste products and its implications for mechanical and thermochemical recycling. Environ Sci Technol 2020;54:13282–93. https://doi.org/10.1021/acs.est.0c03371.
[16] López A, De Marco I, Caballero BM, Laresgoiti MF, Adrados A. Dechlorination of fuels in pyrolysis of PVC containing plastic wastes. Fuel Process Technol 2011;92:253–60. https://doi.org/10.1016/j.fuproc.2010.05.008.

[17] Giglio E, Marino A, Pizarro P, Escola JM, Migliori M, Giordano G, et al. Critical issues for the deployment of plastic waste pyrolysis. Catal Sci Technol 2023;13:5799–820. https://doi.org/10.1039/D3CY00445G.
[18] Tito E, dos Passos JS, Bensaid S, Pirone R, Biller P. Multilayer plastic film chemical recycling via sequential hydrothermal liquefaction. Resour Conserv Recycl 2023;197:107067. https://doi.org/10.1016/j.resconrec.2023.107067.
[19] Jin K, Vozka P, Kilaz G, Chen W-T, Wang N-H-L. Conversion of polyethylene waste into clean fuels and waxes via hydrothermal processing (HTP). Fuel 2020;273:117726. https://doi.org/10.1016/j.fuel.2020.117726.
[20] Goto M. Chemical recycling of plastics using sub- and supercritical fluids. J Supercrit Fluids 2009;47:500–7. https://doi.org/10.1016/j.supflu.2008.10.011.
[21] Poerschmann J, Weiner B, Woszidlo S, Koehler R, Kopinke FD. Hydrothermal carbonization of poly(vinyl chloride). Chemosphere 2015;119:682–9. https://doi.org/10.1016/j.chemosphere.2014.07.058.
[22] dos Passos JS, Glasius M, Biller P. Screening of common synthetic polymers for depolymerization by subcritical hydrothermal liquefaction. Process Saf Environ Prot 2020;139:371–9. https://doi.org/10.1016/j.psep.2020.04.040.
[23] Lu J, Ma S, Gao J. Study on the pressurized hydrolysis dechlorination of PVC. Energy Fuel 2002;16:1251–5. https://doi.org/10.1021/ef020048t.
[24] Salimi M, Pedersen TH, Rosendahl L. Optimizing hydrothermal dechlorination of PVC in a SS-316 reactor: From chemistry knowledge to material considerations. J Environ Chem Eng 2023;11:109783. https://doi.org/10.1016/j.jece.2023.109783.
[25] Ling M, Ma D, Hu X, Liu Z, Wang D, Feng Q. Hydrothermal treatment of polyvinyl chloride: Reactors, dechlorination chemistry, application, and challenges. Chemosphere 2023;316:137718. https://doi.org/10.1016/j.chemosphere.2022.137718.
[26] Zhu Z, Toor SS, Rosendahl L, Yu D, Chen G. Influence of alkali catalyst on product yield and properties via hydrothermal liquefaction of barley straw. Energy 2015;80:284–92. https://doi.org/10.1016/j.energy.2014.11.071.
[27] Gandon-Ros G, Soler A, Aracil I, Gómez-Rico MF. Dechlorination of polyvinyl chloride electric wires by hydrothermal treatment using K2CO3 in subcritical water. Waste Manag 2020;102:204–11. https://doi.org/10.1016/j.wasman.2019.10.050.
[28] Zhao P, Li T, Yan W, Yuan L. Dechlorination of PVC wastes by hydrothermal treatment using alkaline additives. Environ Technol 2018;39:977–85. https://doi.org/10.1080/09593330.2017.1317841.
[29] Biller P, Madsen RB, Klemmer M, Becker J, Iversen BB, Glasius M. Effect of hydrothermal liquefaction aqueous phase recycling on bio- crude yields and composition. Bioresour Technol 2016;220:190–9. https://doi.org/10.1016/j.biortech.2016.08.053.
[30] Channiwala SA, Parikh PP. A unified correlation for estimating HHV of solid, liquid and gaseous fuels. Fuel 2002;81:1051–63. https://doi.org/10.1016/S0016-2361(01)00131-4.
[31] Zhang X. Applications of kinetic methods in thermal analysis: A review. Eng Sci 2021;14:1–13. https://doi.org/10.30919/es8d1132.
[32] Takeshita Y, Kato K, Takahashi K, Sato Y, Nishi S. Basic study on treatment of waste polyvinyl chloride plastics by hydrothermal decomposition in subcritical and supercritical regions. J Supercrit Fluids 2004;31:185–93. https://doi.org/10.1016/j.supflu.2003.10.006.
[33] Lu J, Ma S, Gao J, Freitas JCC, Bonagamba TJ. Study on characterization of pyrolysis and hydrolysis products of poly(vinyl chloride) waste. J Appl Polym Sci 2003;90:3252–9. https://doi.org/10.1002/app.12984.
[34] Nagai Y, Smith RL, Inomata H, Arai K. Direct observation of polyvinylchloride degradation in water at temperatures up to 500°C and at pressures up to 700 MPa. J Appl Polym Sci 2007;106:1075–86. https://doi.org/10.1002/app.26790.
[35] Yoshioka T, Kameda T, Ieshige M, Okuwaki A. Dechlorination behaviour of flexible poly(vinyl chloride) in NaOH/EG solution. Polym Degrad Stab 2008;93:1822–5. https://doi.org/10.1016/j.polymdegradstab.2008.07.009.
[36] Lu J, Borjigin S, Kumagai S, Kameda T, Saito Y, Yoshioka T. Practical dechlorination of polyvinyl chloride wastes in NaOH/ethylene glycol using an up-scale ball mill reactor and validation by discrete element method simulations. Waste Manag 2019;99:31–41. https://doi.org/10.1016/j.wasman.2019.08.034.
[37] Yao Z, Ma X. A new approach to transforming PVC waste into energy via combined hydrothermal carbonization and fast pyrolysis. Energy 2017;141:1156–65. https://doi.org/10.1016/j.energy.2017.10.008.
[38] Ma D, Liang L, Hu E, Chen H, Wang D, He C, et al. Dechlorination of polyvinyl chloride by hydrothermal treatment with cupric ion. Process Saf Environ Prot 2021;146:108–17. https://doi.org/10.1016/j.psep.2020.08.040.
[39] Bodîrlău R, Teacă CA, Spiridon I. Preparation and characterization of composites comprising modified hardwood and wood polymers/poly(vinyl chloride). BioResources 2009;4:1285–304. https://doi.org/10.15376/biores.4.4.1285-1304.
[40] Coltro L, Pitta JB, Madaleno E. Performance evaluation of new plasticizers for stretch PVC films. Polym Test 2013;32:272–8. https://doi.org/10.1016/j.polymertesting.2012.11.009.
[41] Sau S, Pandit S, Kundu S. Crosslinked poly (vinyl alcohol): Structural, optical and mechanical properties. Surf Interfaces 2021;25:101198. https://doi.org/10.1016/j.surfin.2021.101198.
[42] Nandiyanto ABD, Oktiani R, Ragadhita R. How to read and interpret ftir spectroscope of organic material. Indones J Sci Technol 2019;4:97–118. https://doi.org/10.17509/ijost.v4i1.15806.
[43] Yang J, Wu Y, Zhu J, Yang H, Li Y, Jin L, et al. Insight into the pyrolysis behavior of polyvinyl chloride using in situ pyrolysis time-of-flight mass spectrometry: Aromatization mechanism and Cl evolution. Fuel 2023;331:125994. https://doi.org/10.1016/j.fuel.2022.125994.
[44] Wang Z, Wei R, Wang X, He J, Wang J. Pyrolysis and combustion of polyvinyl chloride (PVC) sheath for new and aged cables via thermogravimetric analysis-fourier transform infrared (TG-FTIR) and calorimeter. Materials (Basel) 2018;11. https://doi.org/10.3390/ma11101997.
[45] Hou X, Ma Z, Chen B, Zhang J, Ning Y, Zhao L, et al. Role of normal/cyclo-alkane in hydrocarbons pyrolysis process and product distribution. J Anal Appl Pyrolysis 2021;156:105130. https://doi.org/10.1016/j.jaap.2021.105130.
[46] Cypres R. Aromatic hydrocarbons formation during coal pyrolysis. Fuel Process Technol 1987;15:1–15. https://doi.org/10.1016/0378-3820(87)90030-0.
[47] Fabbri D, Torri C, Spokas KA. Analytical pyrolysis of synthetic chars derived from biomass with potential agronomic application (biochar). Relationships with impacts on microbial carbon dioxide production. J Anal Appl Pyrolysis 2012;93:77–84. https://doi.org/10.1016/j.jaap.2011.09.012.
[48] Zhou J, Liu G, Wang S, Zhang H, Xu F. TG-FTIR and Py-GC/MS study of the pyrolysis mechanism and composition of volatiles from flash pyrolysis of PVC. J Energy Inst 2020;93:2362–70. https://doi.org/10.1016/j.joei.2020.07.009.
[49] Hashimoto K, Suga S, Wakayama Y, Funazukuri T. Hydrothermal dechlorination of PVC in the presence of ammonia. J Mater Sci 2008;43:2457–62. https://doi.org/10.1007/s10853-007-2015-x.
[50] Li Z, Niu S, Liu J, Wang Y. Solid fuel production from co-hydrothermal carbonization of polyvinyl chloride and corncob: Higher dechlorination efficiency and process water recycling. Sci Total Environ 2022;843:157082. https://doi.org/10.1016/j.scitotenv.2022.157082.
[51] Shin S-M, Yoshioka T, Okuwaki A. Dehydrochlorination behavior of flexible PVC pellets in NaOH solutions at elevated temperature. J Appl Polym Sci 1998;67:2171–7. https://doi.org/10.1002/(SICI)1097-4628(19980328)67:13<2171::AID-APP7>3.0.CO;2-B.
[52] Yang M, Zhao P, Cui X, Geng F, Guo Q. Kinetics study on hydrothermal dechlorination of poly(vinyl chloride) by in-situ sampling. Environ Technol Innov 2021;23:101703. https://doi.org/10.1016/j.eti.2021.101703.
[53] Xiu FR, Lu Y, Qi Y. DEHP degradation and dechlorination of polyvinyl chloride waste in subcritical water with alkali and ethanol: A comparative study. Chemosphere 2020;249:126138. https://doi.org/10.1016/j.chemosphere.2020.126138.
[54] Čolnik M, Kotnik P, Knez Ž, Škerget M. Degradation of polyvinyl chloride (PVC) waste with supercritical water. Processes 2022;10:1–14. https://doi.org/10.3390/pr10101940.
[55] Fisch MH, Bacaloglu R. Mechanism of poly(vinyl chloride) stabilisation. Plast Rubber Compos Process Appl 1999;28:119–24. https://doi.org/10.1179/146580199101540213.
[56] Mukherjee AK, Gupta A. Structure and dehydrochlorination of poly(vinyl chloride). J Macromol Sci Part C 1981;20:309–31. https://doi.org/10.1080/00222358108080921.
[57] Bockisch C, Lorance ED, Hartnett HE, Shock EL, Gould IR. Kinetics and mechanisms of dehydration of secondary alcohols under hydrothermal conditions. ACS Earth Sp Chem 2018;2:821–32. https://doi.org/10.1021/acsearthspacechem.8b00030.
[58] Zhao P, Li Z, Li T, Yan W, Ge S. The study of nickel effect on the hydrothermal dechlorination of PVC. J Clean Prod 2017;152:38–46. https://doi.org/10.1016/j.jclepro.2017.03.101.
[59] Li T, Zhao P, Lei M, Li Z. Understanding hydrothermal dechlorination of PVC by focusing on the operating conditions and hydrochar characteristics. Appl Sci 2017;7:256. https://doi.org/10.3390/app7030256.
[60] Tito E, Pipitone G, Monteverde Videla AHA, Bensaid S, Pirone R. Exploring HTL pathways in carbohydrate–protein mixture: A study on glucose–glycine interaction. Biomass Convers Biorefinery 2023;13:16385–404. https://doi.org/10.1007/s13399-023-03967-7.